Ray optical light trapping in silicon microwires: exceeding the $2n^2$ intensity limit

Emily D. Kosten,[1] **Emily L. Warren,**[2] **and Harry A. Atwater**[1,3,*]

[1]*Thomas J. Watson Laboratories of Applied Physics, California Institute of Technology, Pasadena, California 91125, USA*
[2]*Division of Chemistry and Chemical Engineering, California Institute of Technology, Pasadena, California 91125, USA*
[3]*Kavli Nanoscience Institute, California Institute of Technology, Pasadena, California 91125, USA*

*haa@caltech.edu

Abstract: We develop a ray optics model of a silicon wire array geometry in an attempt to understand the very strong absorption previously observed experimentally in these arrays. Our model successfully reproduces the n^2 ergodic limit for wire arrays in free space. Applying this model to a wire array on a Lambertian back reflector, we find an asymptotic increase in light trapping for low filling fractions. In this case, the Lambertian back reflector is acting as a wide acceptance angle concentrator, allowing the array to exceed the ergodic limit in the ray optics regime. While this leads to increased power per volume of silicon, it gives reduced power per unit area of wire array, owing to reduced silicon volume at low filling fractions. Upon comparison with silicon microwire experimental data, our ray optics model gives reasonable agreement with large wire arrays (4 μm radius), but poor agreement with small wire arrays (1 μm radius). This suggests that the very strong absorption observed in small wire arrays, which is not observed in large wire arrays, may be significantly due to wave optical effects.

OCIS codes: (080.0080) Geometric optics; (350.6050) Solar energy; (000.6590) Statistical mechanics; (030.5630) Radiometry; (260.6970) Total internal reflection.

References and links

1. M. Kelzenberg, S. Boettcher, J. Petykiewicz, D. Turner-Evans, M. Putnam, E. Warren, J. Spurgeon, R. Briggs, N. Lewis, and H. Atwater, "Enhanced absorption and carrier collection in si wire arrays for photovoltaic applications," Nat. Mater. **9**, 239–244 (2010).
2. E. Garnett and P. Yang, "Light trapping in silicon nanowire solar cells," Nano Lett. **10**, 1082–1087 (2010).
3. L. Tsakalakos, J. Balch, J. Fronheiser, M. Shih, S. LaBoeuf, M. Pietrzykowski, P. Codella, B. Korevaar, O. Sulima, J. Rand, A. Davuluru, and U. Ropol, "Strong broadband absorption in silicon nanowire arrays with a large lattice constant for photovoltaic applications," J. Nanophoton. **1**, 013552 (2007).
4. B. Tian, X. Zheng, T. Kempa, Y. Fang, J. Huang, and C. Lieber, "Coaxial silicon nanowires as solar cells and nanoelectronic power sources," Nature **449**, 885–889 (2007).
5. E. Garnett and P. Yang, "Silicon nanowire radial p-n junction solar cells," J. Am. Chem. Soc. **130**, 9224–9225 (2008).
6. B. Kayes, H. Atwater, and N. Lewis, "Comparison of the device physics principles of planar and radial p-n junction nanorod solar cells," J. Appl. Phys. **7**, 114302–114311 (2005).
7. M. Putnam, S. Boettcher, M. Kelzenberg, D. Turner-Evans, J. Spurgeon, E. Warren, R. Briggs, N. Lewis, and H. Atwater, "Si microwire-array solar cells," Energy Environ. Sci. **3**, 1037–1041 (2010).

#138520 - $15.00 USD
Received 22 Nov 2010; accepted 25 Jan 2011; published 4 Feb 2011

8. L. Hu and G. Chen, "Analysis of optical absorption in silicon nanowire arrays for photovoltaic applications," Nano Lett. **7**, 3249–3252 (2007).
9. C. Kenrick, H. Yoon, Y. Yuwen, G. Barber, H. Shen, T. Mallouk, E. Dickey, T. Mayer, and J. Redwing, "Radial junction silicon wire array solar cells fabricated by gold-catalyzed vapor-liquid-solid growth," Appl. Phys. Lett. **97**, 143108 (2010).
10. K. Peng and S. Lee, "Silicon nanowires for photovoltaic solar energy conversion," Adv. Mater. **20**, 1–18 (2010).
11. O. Gunawan, K. Wang, B. Fallahazad, Y. Zhang, E. Tutuc, and S. Guha, "High performance wire-array silicon solar cells," Prog. Photovolt. Res. Appl. **10**, 1002 (2010).
12. J. Zhu, Z. Yu, G. Burkhard, C. Hsu, S. Connor, Y. Xu, Q. Wang, M. McGehee, S. Fan, and Y. Cui, "Optical absorption enhancement in amorphous silicon nanowire and nanocone arrays," Nano Lett. **9**, 279–282 (2009).
13. C. Lin and M. Povinelli, "Optical absorption enhancement in silicon nanowire arrays with a large lattice constant for photovoltaic applications," Nano Lett. **7**, 3249–3252 (2007).
14. E. Yablonovitch, "Statistical ray optics," J. Opt. Soc. Am. **72**(7), 899–907 (1982).
15. M. Putnam, D. Turner-Evans, M. Kelzenberg, S. Boettcher, N. Lewis, and H. Atwater, "10 μm minority-carrier diffusion lengths in si wire synthesized by cu-catalyzed vapor-liquid-solid growth," Appl. Phys. Lett. **95**, 163116 (2009).
16. M. Born and E. Wolf, *Principles of Optics, 7th Ed.* (Cambridge University Press, 1999).
17. We find our model very slightly exceeds the ergodic limit across all aspect ratios for the smallest filling fraction. This is observed across aspect ratios, with no trend with increasing aspect ratios. The maximum amount by which the ergodic limit is exceeded is approximately 1% and is likely due to small inaccuracies in the model.
18. This should not be confused with the areal filling fraction of the wire array. In solar cells, the power can be calculated by multiplying the short circuit current, the open circuit voltage, and the fill factor, where the fill factor accounts for the fact that the current-voltage curve is not square in the power-producing region.
19. K. Plass, M. Filler, J. Spurgeon, B. Kayes, S. Maldonado, B. Brunschwig, H. Atwater, and N. Lewis, "Flexible polymer-embedded si wire arrays," Adv. Mater. **21**, 325–328 (2009).
20. C. Bohren and D. Huffman, *Absorption and Scattering of Light by Small Particles* (Wiley-VCH, 2004).

1. Introduction

Silicon nanowire and microwire arrays have attracted significant interest as an alternative to traditional wafer-based technologies for solar cell applications [1–12] . Originally, this interest stemmed from the device physics advantages of a radial junction, which allows for the decoupling of the absorption length from the carrier collection length. In a planar cell, both of these lengths correspond to the thickness of the cell, and high quality material is necessary so that the cell can absorb most of the light while successfully collecting the carriers. In contrast, a radial junction offers the possibility of using lower quality, lower cost materials without sacrificing performance [5, 6]. More recently, such arrays have been found to exhibit significant light trapping and absorption properties [1–3], and this absorption has been modeled using the transfer matrix formalism in the nanowire regime [8, 13].

Enhancing the light trapping and absorption within a solar cell leads to increased production of electron hole pairs, and a corresponding increase in short circuit current. Light trapping schemes, such as texturing, are particularly important in the case of silicon and other low absorbing materials. For textured planar substrates in the ray optics regime the light trapping limit under isotropic illumination will be referred to here as the ergodic limit. In this limit, the intensity of light inside the substrate is n^2 times the intensity of light incident upon the substrate, or $2n^2$ for the case of a back-reflector, where n is the index of refraction for the substrate. This effect is due to the randomizing effect of the texturing and total internal reflection [14]. Some very recent experimental results have suggested that nano and microwire arrays can exceed the ergodic limit [1, 2]. To explore this further, we follow the approach used to derive the ergodic limit in the planar case to find the expected light trapping and absorption for wires in the ray optics limit. This allows us to compare to the ergodic limit and consider wires of a different scale than those considered in previously.

While much of the previous work has been done with nanowires in the subwavelength regime, far below the ray optics limit, large diameter microwires can be grown by vapor-liquid-solid (VLS) techniques [1]. Previous device physics modeling suggests that for efficient car-

#138520 - $15.00 USD Received 22 Nov 2010; accepted 25 Jan 2011; published 4 Feb 2011

rier collection wires should have diameters similar to the minority carrier diffusion length, [6] and experimental measurements show diffusion lengths for VLS grown microwires of 10 microns [15]. Because wires with such diameters could approach the ray optics limit for solar wavelengths, it seems sensible to model these structures in the ray optics regime. In addition, comparison of the ray optics model with experimental data provides insight into the relative importance of wave optics effects for wires of various diameters.

We begin by assuming there is no absorption in the wires and examine the case for isotropic illumination so that we can compare to the ergodic light trapping limit for textured, weakly absorbing, planar dielectric substrates. To make this comparison, it is also necessary to postulate textured surfaces for the wires. We then examine the case of wires on a Lambertian back reflector, which are illuminated isotropically over the upper half sphere. Finally, we add a weak absorption term and find the absorption as a function of wavelength and angle of incidence, allowing us to compare with experimental data.

2. Modeling wire array intensity enhancement under isotropic illumination

We base our model on the principle of detailed balance, as was done to derive the ergodic limit for textured planar sheets [14]. In detailed balance, the light escaping from the wires is set equal to the light entering the wires. To illustrate our approach and show proof of concept for the model, we first imagine a hexagonal array of wires suspended in free space and isotropically illuminated. Furthermore, we assume that the wire surfaces are roughened such that they act as Lambertian scatterers. In other words, the brightness of the wire surfaces will be equal regardless of the angle of observation [16]. This fully randomizes the light inside the wires in the limit of low absorption, just as the roughened surfaces of planar solar cells do. The randomization of light within the wires serves to trap the light inside by total internal reflection.

With these assumptions in mind, we find the governing equation by simply balancing the inflows and outflows of light within a single wire.

$$I_{inc} 2A_{end} \bar{T}_{end} + I_{inc} A_{sides} \bar{F} = \frac{I_{int} 2A_{end} \bar{T}_{end}}{n^2} + \frac{I_{int} A_{sides} \bar{L}}{n^2} \tag{1}$$

Above, I_{inc} is the intensity of the incident radiation, I_{int} is the the intensity of light within the wires, A_{sides} is the area of the wires sides, A_{end} is the area of one wire end, and n is the index of refraction of the wire. In addition, $\bar{T}_{end}$ is the average transmission factor through the end, $\bar{L}$ is light from the sides which escapes the array, and $\bar{F}$ is the incident light which enters through the sides.

The terms on the left hand side represent the energy entering the wire array, with the two terms representing the incident light which enters through the side and tops of the wire respectively. For the top of the wire, the calculation is quite simple because there is no shadowing or multiple scattering, assuming that the wires are all the same height. Thus, we only need to average the transmission into the top over the incident angles to find $\bar{T}_{end}$. For light entering through the sides, we take into account transmission into the wire in addition to shadowing and multiple scattering. Thus, for a given incident angle, we determine $\bar{F}$, which gives the fraction of light transmitted through the sides, averaged over the angles of the incident radiation.

On the right hand side, we have the energy outflows. Once again, the outflows from the top are quite simple, as all light that leaves the top is lost to the array. The factor of $1/n^2$, is due to total internal reflection of the randomized light inside the wire, as Yablonovitch previously demonstrated for ergodic structures [14]. Due to the isotropic incident radiation, the averaged transmission fractor T_{end} is the same for incident and escaping light. For losses through the sides, much of the emitted light will be transmitted into other wires, and not lost from the array. Thus, an average loss factor, $\bar{L}$, is found, which gives the side losses which are not transmitted

#138520 - $15.00 USD Received 22 Nov 2010; accepted 25 Jan 2011; published 4 Feb 2011

into other wires.

We rearrange the above equation to find the degree of light-trapping, or I_{int}/I_{inc}.

$$\frac{I_{int}}{I_{inc}} = \frac{n^2(2A_{end}\bar{T}_{end} + A_{sides}\bar{F})}{2A_{end}T_{end} + A_{sides}\bar{L}} \tag{2}$$

Note, that in the limit where the area of the sides goes to zero, the light trapping factor is n^2, which reproduces the ergodic limit for a planar textured sheet, isotropically illuminated, as we expect. If $\bar{F}$ is larger than $\bar{L}$, the light trapping in this structure could exceed the ergodic limit. This seems unlikely, however, as time-reversal invariance would suggest that $\bar{L} = \bar{F}$ because each path into the array much also be an equally efficient path out of the array. Furthermore, from a thermodynamics perspective, we expect that the light trapping in this structure should be exactly n^2. This is because the equipartition theorem states that all the states or modes should be equally occupied in thermodynamic equilibrium, and the density of states is n^3 the of states in free space. (When calculating the intensity, it is necessary to multiply by the group velocity which goes as $1/n$, such that the intensity is increased by n^2) [14]. Thus, this case will allow us to assess the accuracy of the model and the assumptions necessary to simplify the calculation.

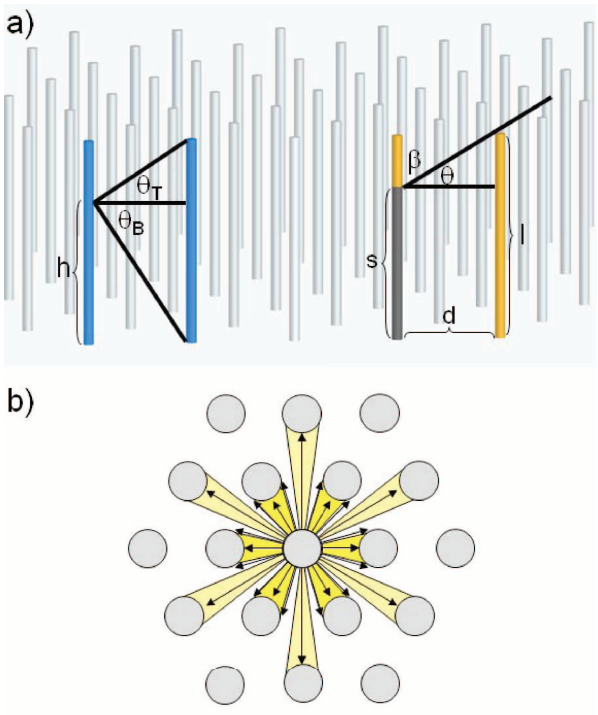

Fig. 1. (a) Schematic of the wire array for isotropic illumination. The blue wires illustrate how light escaping from the side of a wire impinges on a neighboring wire a given distance away. The orange wires illustrate how the sides of the wires are shadowed by neighboring wires for a given distance and angle of incidence. (b) A top-down view of the wire array illustrates the radial escape approximation. The arrows show the directions of light escape being considered, and the yellow areas give the in-plane angle subtended by the neighboring wires, with the distinct shades indicating neighboring wires at two distinct distances. The wires farther away will have greater loss associated than the closer wires.

#138520 - $15.00 USD Received 22 Nov 2010; accepted 25 Jan 2011; published 4 Feb 2011

Averaging over all solid angles, with an appropriate intensity weighting gives, $\bar{T}_{end}$:

$$\bar{T}_{end} = \frac{\int_0^{2\pi}\int_0^{\pi/2} T(\phi)\cos(\phi)\sin(\phi)\, d\phi\, d\theta}{\int_0^{2\pi}\int_0^{\pi/2}\cos(\phi)\sin(\phi)\, d\phi\, d\theta} = \frac{\int_0^{2\pi}\int_0^{\pi/2} T_n\cos^2(\phi)\sin(\phi)\, d\phi\, d\theta}{\int_0^{2\pi}\int_0^{\pi/2}\cos(\phi)\sin(\phi)\, d\phi\, d\theta} = \frac{2}{3}T_n \quad (3)$$

where ϕ is the angle of incidence and T_n is the transmission factor at normal incidence, and where we have used the transmission factor associated with a Lambertian surface ($T_n\cos(\phi)$) [16].

To calculate $\bar{L}$, we determine the fraction of light, g, escaping from the sides of a given wire that impinges on neighboring wires. Then, we determine the transmission into those neighboring wires and the effect of multiple scattering from neighboring wires. To find g, we invoke a radial escape approximation where we treat each wire as if it were a line extending upward from the plane of the array. This approximation will be more accurate for low filling fraction arrays, because with greater distance between the wires means that neighboring wires more closely approximate line sources. The radial escape approximation serves to significantly simplify the treatment of the in-plane shadowing. With this assumption, we only need to calculate the portion of the in-plane angle that is subtended by wires at a given distance, and the losses associated with each distance in order to find g. As Fig. 1(b) illustrates, the in-plane angle subtended by neighboring wires at a given distance is calculated geometrically.

The fraction of light that impinges on a wire a given distance away, $f(h)$ is easily calculated from geometrical arguments and the properties of Lambertian surfaces, as Fig. 1(a) illustrates. To simplify the calculation we ignore the increase in wire to wire distance as the wires curve away from each other. As before, this approximation will be more accurate for lower filling fractions, where the wires are farther apart and this effect will be smaller.

$$f(h) = \frac{\int_{-\theta_B}^{\theta_T}\cos(\theta)d\theta}{\int_{-\pi/2}^{\pi/2}\cos(\theta)d\theta} = \frac{\sin(\theta_T)+\sin(\theta_B)}{2} \quad (4)$$

To find $g(d)$, we integrate $f(h)$ over the height of the wire and normalize.

$$g(d) = \frac{\int_0^{l}\sin(\theta_T)+\sin(\theta_B)dh}{2l} = \frac{\sqrt{l^2+d^2}-d}{l} \quad (5)$$

Then, g is an average of $g(d)$ weighted by the angles subtended at each distance.

Naturally, not all of the light which strikes a neighboring wire will be transmitted into the wire. As before, we calculate a transmission factor as a function of distance, $T_{int}(d)$ and take a weighted average to find the overall internal transmission factor, T_{int}. Here, however, we must account for the curvature of the wire because this significantly affects the angle the transmitted light makes with the wire surface. Assuming equal brightness for the allowed in plane and out of plane angles, the expression for $T_{int}(d)$ is:

$$T_{int}(d) = \frac{\int_0^{l}\int_{-\theta_B}^{\theta_T}\int_{-\alpha_1}^{\alpha_2} T_n\cos^2(\phi)d\alpha d\theta dl}{\int_0^{l}\int_{-\theta_B}^{\theta_T}\int_{-\alpha_1}^{\alpha_2}\cos(\phi)d\alpha d\theta dl} \quad (6)$$

where the θ's give the bounds of the out of plane angles, the α's the bounds of the in-plane angles, and ϕ is the overall angle made with the wire.

To find $\bar{L}$ we sum the losses in each pass through the wire array. For the first pass through the wire array, $1-g$ of light which left the wire side is lost, because it does not impinge on any of the other wires, and escapes. This is multiplied by $\bar{T}_{end}$ because the light must leave the side of

#138520 - $15.00 USD Received 22 Nov 2010; accepted 25 Jan 2011; published 4 Feb 2011

the wire before it can escape the array. On the second pass, the losses, L_2, are as follows:

$$L_2 = \bar{T}_{end} g(1-T_{int})(1-g) \tag{7}$$

This assumes that the reflected light has a uniform height distribution. In reality, more of the light emitted from the sides of the wires will impinge on the middle of the neighboring wire than either end, owing to the Lambertian distribution of light from the emitting wire. Thus, this assumption will overestimate the losses on succeeding passes through the array, but greatly reduces the computational intensity of the calculation by allowing for a generalization of the losses on the *i*th pass through the array as:

$$L_i = \bar{T}_{end}(g(1-T_{int}))^{i-1}(1-g) \tag{8}$$

This can easily be summed to give $\bar{L}$.

$$\bar{L} = \bar{T}_{end}(1-g)\sum_{n=0}^{\infty}(g(1-T_{int}))^n = \frac{1-g}{1-g(1-T_{int})} \tag{9}$$

In calculating $\bar{F}$ the main additional phenomenon we must address is shadowing. As Fig. 1(a) illustrates, the shadowing fraction, u, as a function of wire to wire distance and angle of incidence is:

$$u(d,\beta) = \frac{l-s}{l} = \frac{d\cot(\beta)}{l} \tag{10}$$

We then take a weighted average over the angle subtended at each distance to find $u(\beta)$, and also find the transmission factor for the incoming light as a function of β by averaging over all in-plane angles α.

$$T_0(\beta) = \frac{\int_{-\pi/2}^{\pi/2} T_n \cos^2(\phi) d\alpha}{\int_{-\pi/2}^{\pi/2} \cos(\phi) d\alpha} \tag{11}$$

As before ϕ is the overall angle the incoming ray makes with the wire, which will depend on both α and β. Finally, we modify the multiple scattering model because light will only be reflected off the unshadowed portion of the wire, which will vary as a function of β. For the losses on the first pass through the array:

$$L_1(\beta) = u(\beta)(1-T_0(\beta))(1-g_1(\beta)) \tag{12}$$

For $i > 1$,

$$L_i(\beta) = (1-g)u(\beta)(1-T_0(\beta))g_1(\beta)(1-T_1(\beta))[g(1-T_{int})]^{i-2} \tag{13}$$

where L_i gives the losses on the *i*th bounce, as before, and T_1 and g_1 give the transmission and impingement factors associated with the light reflected from the unshadowed portion of the wires. Summing to find the total losses:

$$L_t(\beta) = u(\beta)(1-T_0(\beta))\left(1-g_1(\beta)+\frac{(1-g)g_1(\beta)(1-T_1(\beta))}{1-g(1-T_{int})}\right) \tag{14}$$

Thus, for a given angle, β, the amount of light which is transmitted into the wires, $F(\beta)$, accounting for multiple scattering and shadowing is:

$$F(\beta) = u(\beta) - L_t(\beta) \tag{15}$$

#138520 - $15.00 USD Received 22 Nov 2010; accepted 25 Jan 2011; published 4 Feb 2011

Averaging over all the angles of incidence gives $\bar{F}$.

$$\bar{F} = \frac{\int_0^{2\pi}\int_0^{\pi/2} F(\beta)\sin^2(\beta)d\beta d\eta}{\int_0^{2\pi}\int_0^{\pi/2}\sin^2(\beta)d\beta d\eta} \tag{16}$$

Above, η is the polar angle, $\sin(\beta)d\beta d\eta$ is the differential solid angle, and the additional factor of sine gives the change in intensity with angle of incidence.

3. Results for wire array intensity enhancement under isotropic illumination

Inserting the expressions found above into Eq. (2), we calculate the light trapping factor across a range of areal filling fractions, the fraction of the array covered by wires, for various wire aspect ratios. The results are given in Fig. 2 and are indicated by the curves labeled "no back reflector". For very large filling fractions we approach the ergodic limit, because the terms involving the wire sides become very small. We also reproduce the ergodic for very low filling fractions, where the radial escape approximation will be most accurate [17]. In between the results fall below the ergodic limit, likely because the side loss factor, $\bar{L}$, is overestimated in the radial escape approximation. Because we expect thermodynamically that the result should be n^2, this suggests that our approximations are reasonable, especially for low filling fractions, which are more likely to be of experimental interest. We also note that our results are closer to the ergodic limit for smaller aspect ratios. This is likely because the terms involving the wire sides are relatively smaller, and thus inaccuracies in those terms, such as overestimating $\bar{L}$, will have less impact. Thus, our approach reasonably approximates the result we expect from thermodynamics, and the inaccuracies introduced by the radial escape approximation are well understood.

4. Modeling wire array intensity enhancement with a Lambertian back reflector

We now investigate the effect of having a Lambertian back reflector with isotropic illumination in the upper half-sphere. In this case, no light will enter or escape through the bottom ends of the wires, which are covered by the back-reflector, and light that strikes the reflector will be scattered. In the planar case, the ergodic light trapping limit for such a geometry is $2n^2$, owing to the back reflector. Additionally, it seems that this geometry would give optimal scattering, as can be understood by basic physical arguments. Experimentally, it has been found that placing scatterers within the wire array can, in combination with a back-reflector, improve the performance of the array [1, 7]. This is because scatterers prevent light which is at normal or nearly normal incidence from going between the wires and bouncing off a planar back-reflector and out of the array. Imagine that we could place scatterers at any height level within the wire array. The light that scatters upward from the scatterers near the bottom of the array will be more likely to impinge on a wire, as Fig. 3 shows. For optimal scattering, then, the scatterers should be placed at the bottom of the array. Since a Lambertian back reflector is similar to placing scatterers on a planar back reflector, this geometry allows us to investigate an optimal scattering regime as well as providing an interesting comparison to the planar case.

The governing equation for this case once again relies on detailed balance, as shown below.

$$I_{inc}A_{end}\bar{T}_{end} + I_{inc}A_{sides}\bar{F'} + I_{inc}A_{refl}\bar{R'} = \frac{I_{int}A_{end}\bar{T}_{end}}{2n^2} + \frac{I_{int}A_{sides}\bar{L'}}{2n^2} \tag{17}$$

The terms on the left give the light entering a wire, and the terms on the right give the amount of light escaping. Note that a factor of $1/2n^2$ replaces the $1/n^2$ factor because the back reflector doubles the intensity of the light within the wires [14]. In addition, $\bar{L}$ and $\bar{F}$ are replaced with $\bar{L'}$

#138520 - $15.00 USD Received 22 Nov 2010; accepted 25 Jan 2011; published 4 Feb 2011

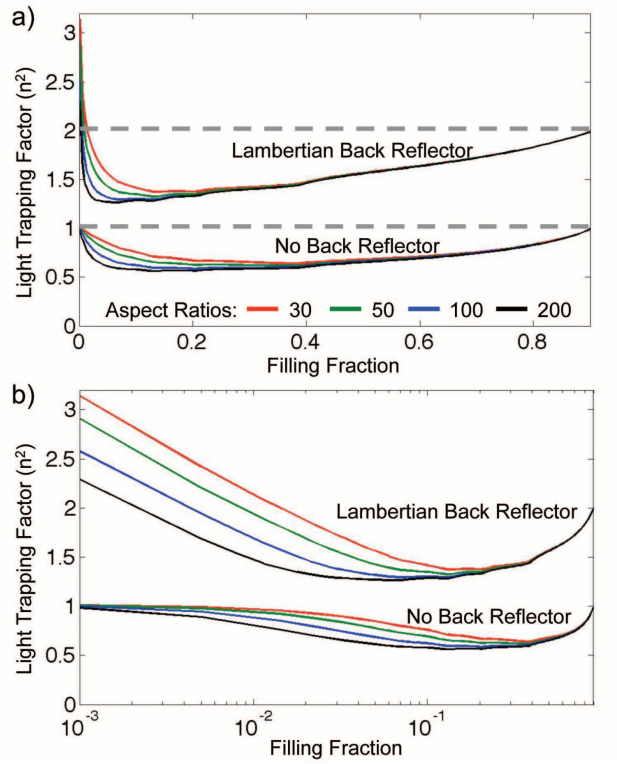

Fig. 2. The variation of the light trapping factor, as a multiple of n^2, as a function of areal filling fraction, for various aspect ratios (height/radius). n=3.53. Because we assume a cylindrical wire geometry, the maximum attainable packing fraction is approximately 90%, which corresponds to the sides of the wires touching each other. The minimum filling fraction shown is 0.1%. Both cases approach their respective ergodic limits (denoted by gray dashed lines) for large filling fractions. The no back reflector case is also very close to the ergodic limit for very small filling fractions where the radial escape approximation is accurate. Parts a and b show the same data plotted against a linear and log scale.

and $\bar{F}'$, indicating that we need to account for the Lambertian back reflector when calculating them. Finally, we note that there is a term accounting for the light that initially falls between the wires and strikes the reflector. $\bar{R}'$ gives the fraction of the light which initially strikes the back reflector that subsequently enters a wire, accounting for shadowing and multiple scattering. With a one wire unit cell, A_{refl}, is simply the reflector area associated with a single wire. As before, we rearrange the above equation to find the relative intensities inside and outside the wire.

$$\frac{I_{int}}{I_{inc}} = \frac{2n^2(A_{end}\bar{T}_{end} + A_{sides}\bar{F}' + A_{refl}\bar{R}')}{A_{end}\bar{T}_{end} + A_{sides}L'} \tag{18}$$

Once again, in the limit of zero side area, the light trapping reduces to the planar ergodic limit of $2n^2$, as expected.

To find the appropriate expressions for $\bar{L}'$ we note that g and T_{int} will both be modified by the back reflector. Therefore, using the modified values of these, g' and T'_{int}, in our previous multiple scattering model gives $\bar{L}'$. To find g', we tally the light lost. Half of the losses from the non-reflector case remain, corresponding to the light that escapes from the top. The other half

#138520 - $15.00 USD Received 22 Nov 2010; accepted 25 Jan 2011; published 4 Feb 2011

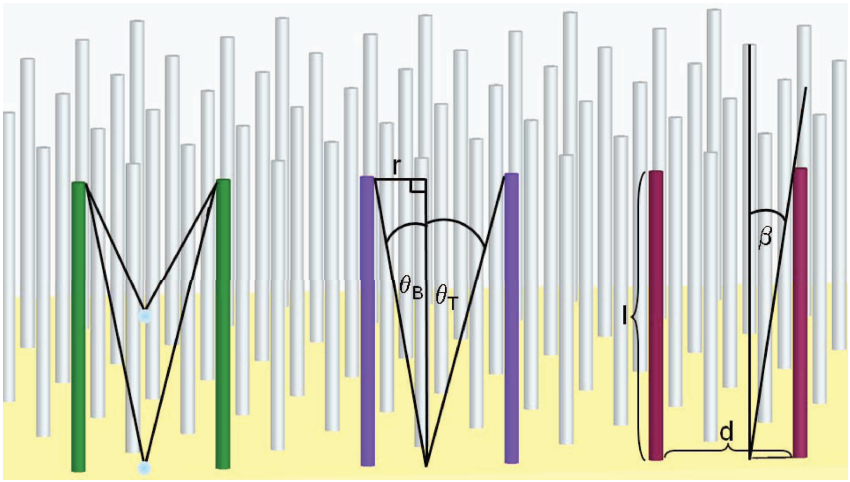

Fig. 3. A schematic of the Lambertian back reflector case. The green wires show the effects of scatterers placed at different heights within the array. Note that for the lower scatterer light from a much smaller range of angles is able to escape. The purple wires illustrate the light which bounces off the reflector at a given point r that escapes between the surrounding wires. Between the red wires the shadowing of the reflector for incident light at a given angle and wires at a given distance is shown.

of the non-reflector losses are multiplied by the losses associated with light bouncing off the reflector and not striking a wire, L_{refl}.

$$1-g' = (1-g)/2 + (1-g)/2 * L_{refl} \tag{19}$$

As Fig. 3 illustrates, we consider two wires a distance d apart, and of height l, with the light being reflected from a point r on the reflector. The fraction of light which escapes at a given location on the reflector will be

$$L(r) = \frac{\int_{-\theta_B}^{\theta_T} \cos(\theta) d\theta}{\int_{-\pi/2}^{\pi/2} \cos(\theta) d\theta} = \frac{\sin(\tan^{-1}(r/l)) + \sin(\tan^{-1}((d-r)/l))}{2} = \frac{\frac{r}{\sqrt{r^2+l^2}} + \frac{d-r}{\sqrt{(d-r)^2+l^2}}}{2} \tag{20}$$

where, as before, we have ignored the curvature of the wires. However, the intensity of light incident on the reflectors will not be constant across the reflector. The intensity at a given point r is be the light coming from all points along the two neighboring wires, accounting for the Lambertian nature of the wire surfaces is:

$$I(r) = \int_0^l \cos(\eta_1) dh + \int_0^l \cos(\eta_2) dh = \int_0^l \frac{r}{\sqrt{r^2+h^2}} dh + \int_0^l \frac{d-r}{\sqrt{(d-r)^2+h^2}} dh \tag{21}$$

where η_1 is the angle to the horizontal made by a ray escaping the wire at a height h to strike the reflector at a point r, and η_2 is the same quantity for the other wire. Averaging over all the points between the two wires, with the appropriate intensity weighting gives:

$$L_{refl}(d) = \frac{\int_0^d I(r) \left[\frac{r}{\sqrt{r^2+l^2}} + \frac{d-r}{\sqrt{(d-r)^2+l^2}} \right] dr}{2 \int_0^d I(r) dr} \tag{22}$$

#138520 - $15.00 USD
Received 22 Nov 2010; accepted 25 Jan 2011; published 4 Feb 2011

$L_{refl}(d)$ is inserted into Eq. (19) to find $g'(d)$. We then take a weighted average of $g'(d)$ with respect to the angle subtended at each distance to find g'.

To find T'_{int} we note that light which impinges without striking the back reflector has a transmission factor which remains unchanged from the non-reflector case. Thus, once the transmission factor for light which bounces off the back reflector is calculated, these two transmission factors can be appropriately weighted together to give an overall transmission factor.

The approach to finding the transmission factor for light that has bounced off the back reflector is similar the the approach for finding the transmission factor for incident side light. Thus, we take $T_0(\beta)$ (see Eq. (11)), and weight it by the cosine dependence associated with the back reflector. Finally, we average over the position along the reflector with a weighting to account for the varying intensity, as shown below.

$$T_{refl}(d) = \frac{\int_0^d I(r)\left(\int_{\theta_T}^{\pi/2}\int_{-\pi/2}^{\pi/2} T_n \cos(\theta)\cos^2(\phi)d\alpha d\theta + \int_{\theta_B}^{\pi/2}\int_{-\pi/2}^{\pi/2} T_n \cos(\theta)\cos^2(\phi)d\alpha d\theta\right)dr}{\int_0^d I(r)\left(\int_{\theta_T}^{\pi/2}\int_{-\pi/2}^{\pi/2} \cos(\phi)\cos(\theta)d\alpha d\theta + \int_{\theta_B}^{\pi/2}\int_{-\pi/2}^{\pi/2} \cos(\phi)\cos(\theta)d\alpha d\theta\right)dr} \tag{23}$$

Since, $g' - g$ is the additional light impingement which results from light which has struck the back reflector, we find:

$$T'_{int}(d) = \frac{g(d)T_{int}(d) + (g'(d) - g(d))T_{refl}(d)}{g'} \tag{24}$$

Then, the overall T'_{int} is a weighted average with the in-plane angles subtended at each distance. Finally, g' and T'_{int} are used in place of their unprimed counterparts in the multiple scattering model (see Eq. (9)) to find $\bar{L}'$.

To find F' we insert g' and T'_{int} in the multiple scattering model in place of their unprimed counterparts. However, as Eq. (14) shows, we also need to find T'_1 and g'_1 To find g'_1 we estimate the impact of the reflector, R, using the following expression:

$$R = (1 - g_1(d)) - (1 - g(d))/2 \tag{25}$$

This estimates the amount of light that would be lost, but instead strikes the reflector. Because the top part will always be shadowed last, we assume the losses from the top are constant and equal $(1-g(d))/2$. Thus, everything else will strike the reflector, and we use our previous result for L_{refl} to find the total losses, $1-g'_1(d)$.

$$1 - g'_1(d) = R * L_{refl} + (1 - g(d))/2 \tag{26}$$

This allows us to modify the transmission factor:

$$T'_1(d) = \frac{T_1(d)g_1(d) + T_{refl}(d)(g'_1(d) - g_1(d))}{g'_1(d)} \tag{27}$$

Inserting all the primed quantities for their unprimed counterparts in the equation for $\bar{F}$, and dividing by two to account for the hemispherical illumination gives F'. Obviously, the shadowing fraction, u, and the transmission factor prior to any reflection, T_0, are unchanged by the presence of the reflector since the sun is directly striking the wire.

To find R', we first determine the shadowing of the reflector as a function of wire to wire

#138520 - $15.00 USD Received 22 Nov 2010; accepted 25 Jan 2011; published 4 Feb 2011

distance and angle of incidence. From Fig. 3, the shadowed fraction of the reflector $u(d,\beta)$ is:

$$u(d,\beta) = \frac{d - l\tan(\beta)}{d} \tag{28}$$

Taking a weighted average with respect to angle subtended at a given distance gives $u(\beta)$, we average over all β's, including the differential solid angle and a weighting for intensity, to find u.

$$u = \frac{\int_0^{\pi/2} u(\beta)\sin(\beta)\cos(\beta)d\beta}{\int_0^{\pi/2} \sin(\beta)\cos(\beta)d\beta} \tag{29}$$

Next we develop a multiple scattering model. The losses from light that doesn't hit a wire after the initial reflection is L_{inc}, which we find by averaging $L(r)$ over the unshadowed portion of the reflector at each distance, with appropriate weighting for shadowing and the angle subtended at each distance. T_{inc}, the transmission of light after initial reflection, is found in an exactly analogous manner. $(1-L_{inc})(1-T_{inc})$ is reflected back into the array after bouncing once off the wire. From the previous result, $(1-g')/(1-g'(1-T'_{int}))$ of this light will be lost. Thus, the total losses for light that initially strikes the reflector are:

$$L_{tot} = L_{inc} + (1-L_{inc})(1-T_{inc})\frac{1-g'}{1-g'(1-T'_{int})} \tag{30}$$

Then,

$$\bar{R'} = (1-L_{tot})u \tag{31}$$

To find $\bar{R'}$, we have approximated the the shadowing of the reflector using the closest distance between two wires, leading to an overestimation of the shadowing impact, which should be larger for high filling fractions. This is consistent with our use of the closest distance between two wires for wire to wire shadowing and and losses.

5. Results for wire array intensity enhancement with a Lambertian back reflector

Inserting the terms derived above into Eq. (18), we find the light trapping factor, which is plotted as a function of filling fraction in Fig. 2 by the curves labeled "Lambertian back reflector". The results closely approach the relevant ergodic limit of $2n^2$ for large filling fractions as the terms involving the wire sides and the reflector become very small. As in the no back reflector case, the light trapping factor falls below the ergodic limit as the filling fraction is decreased from the maximum. It seems likely that, as before, the overestimation of $\bar{L}$ in the radial escape approximation for these filling fractions is at least partially responsible for the decrease. This is supported by the trend in aspect ratios, which is similar to that for the no back reflector case.

Interestingly, we see that for small filling fractions, the light trapping increases asymptotically, significantly exceeding the ergodic limit, in contrast to the no back reflector case. As we previously noted, our approximations improve with decreasing filling fractions. Thus, there is no reason to suspect that surpassing the ergodic limit is an artifact of the modeling assumptions. Furthermore, we can understand the observed asymptotic increase physically by considering the limit of small filling fraction. For very small filling fractions the side loss factor, $\bar{L'}$, and the side transmission factor, $\bar{F'}$, are nearly constant, as they have nearly reached their maxima. In addition, the radius is rapidly approaching zero. Thus, all the terms in Eq. (18), with the exception of the back reflector term, are decreasing as the square of the radius. However, the reflector area remains nearly constant with decreasing filling fraction, as the array is already almost entirely reflector. Thus, if $\bar{R'}$ is decreasing less quickly than the radius squared, we should see asymptotic increase. In fact, fitting the asymptotic regions of each of the curves we find

#138520 - $15.00 USD Received 22 Nov 2010; accepted 25 Jan 2011; published 4 Feb 2011

that the curves are increasing as r^{-p}, where p has values between 0.33 and 0.37. Figure 4 uses the fit in the calculation of the power, to give a sense of the goodness of the fit. The fits are quite good across all the curves, and the values of p do not trend with aspect ratio. These fits suggests that the back reflector transmission goes approximately as the radius to the 5/3 power in the low filling fraction regime, across the range of aspect ratios explored here. The variation of the onset of asymptotic behavior with aspect ratio is also consistent with this explanation, as the denominator of the light trapping factor will decrease more rapidly for shorter wires.

To explore this further, we evaluated the relative power, per unit area and per unit volume of silicon, for an array with an aspect ratio of 50. We assume constant solar cell fill factor [18] with increasing filling fraction, and assume that the short circuit current is proportional to the volume and the light trapping factor. For an axial junction, the open circuit voltage is proportional to $\ln(J_{sc}/J_0)$, where J_{sc} is the short circuit current density and J_0 is the saturation current. We assume that for a light trapping factor of $2n^2$ the short circuit current density is 30 mA/cm^2 and the saturation current density is 10^{-12} A/cm^2. As Fig. 4 illustrates, while the asymptotic increase does produce an increase in power per unit volume of silicon, as we expect, it does not produce an increase in the power per unit area. This is because the reduced volume of silicon per unit area leads to a reduced short circuit current, which is not overcome by the relatively small increase in open circuit voltage. Thus, in some sense, the Lambertian back reflector is acting as a concentrator with an acceptance angle of 2π steradian, leading to increased power per unit volume of silicon at the cost of power per unit area.

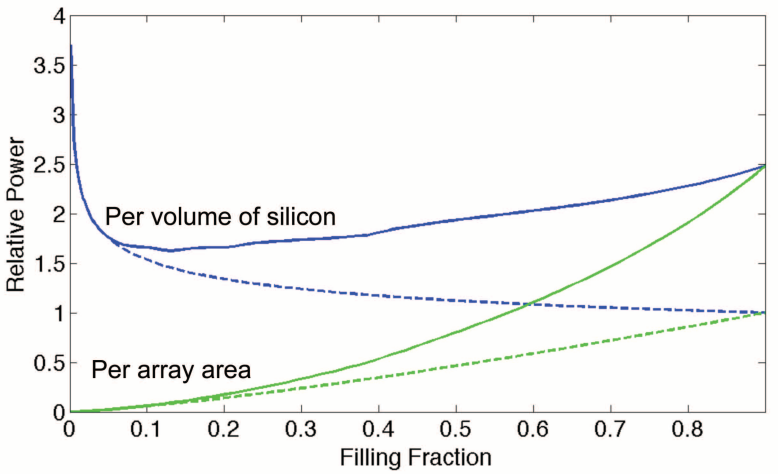

Fig. 4. The variation of power with filling fraction, for aspect ratio=50. The dotted lines use the asymptotic fits across all filling fractions, so that the goodness of fit can be evaluated. The solid lines use the model results across all filling fractions. Note that while the asymptotic increase produces increased power per volume of silicon it does not produce increased power per unit area in the array.

6. Comparison with experiment

Absorption measurements have been reported as a function of angle of incidence and wavelenth for VLS-grown microwire arrays [1]. We therefore calculate the absorption for such an array in the ray optics limit. This will give us insight as to the importance of wave optic effects, and will allow us to determine the accuracy of the model for arrays at various scales. We consider an array embedded in PDMS, with a quartz slide underneath it. This very similar to the non-

#138520 - $15.00 USD
Received 22 Nov 2010; accepted 25 Jan 2011; published 4 Feb 2011

reflector case, except for the fact that we have PDMS/quartz (n=1.4) instead of free space. In addition, we include an absorption term in the governing equation. As Yablonovitch has shown, this term should be equal to $2\alpha V I_{int}$ where α is the absorption coefficient, and V is the volume where the absorption is occurring [14].

Thus, the governing equation for a given angle of incidence θ, is:

$$A'_{sides} I_{max} \sin(\theta) F(\theta) + 2A_{end} I_{max} \cos(\theta) T(\theta) = 2\alpha V I_{int} + \frac{2A_{end}\overline{T}_{end} I_{int}}{n^2} + \frac{A_{sides}\overline{L} I_{int}}{n^2} \quad (32)$$

where I_{max} is the intensity of the incident light at normal incidence, and the factors of $\sin(\theta)$ and $\cos(\theta)$, account for the decreased intensity at non-normal incidence. Note that for the light entering through the sides we have A'_{sides} instead a A_{sides}, to denote that we need to account for decreased intensity as the wire turns away from the in-plane direction from which the light enters. Rearranging to find I_{int} gives:

$$I_{int} = \frac{A'_{sides} I_{max} \sin(\theta) F(\theta) + 2A_{end} I_{max} \cos(\theta) T(\theta)}{2\alpha V + \frac{2A_{end}\overline{T}_{end}}{n^2} + \frac{A_{sides}\overline{L}}{n^2}} \quad (33)$$

The fraction of light absorbed, A, is:

$$A = \frac{2\alpha V I_{int}}{A_{tot} I_{max} \cos(\theta)} = \frac{2\alpha V (A'_{sides} F(\theta) \tan(\theta) + 2A_{end} T(\theta))}{A_{tot}(2\alpha V + \frac{2A_{end}\overline{T}_{end}}{n^2} + \frac{A_{sides}\overline{L}}{n^2})} \quad (34)$$

where A_{tot} is the total area of one unit cell. With the exception of A'_{sides}, these terms follow directly from our previous work. However, between various in plane angles, the amount of shadowing will vary. Previously, to find $\overline{F}$ we averaged this over all the in-plane angles. Experimentally, though, the light will only come from one in-plane direction, which, in this case, was aligned in the direction of maximal shadowing. In addition, to account for a non-free space medium, all the factors of $1/n^2$ are replaced with n_1^2/n_2^2, where n_1 is the index of the embedding medium and n_2 is the index of the wires, due to the relative density of modes between the two media.

To find the experimental absorption data, arrays of silicon microwires were grown by the VLS mechanism from $SiCl_4$ precursors as reported previously [19]. The geometry of the arrays was defined by the photolithographic mask used to pattern the VLS catalyst islands. Wires with a radius of 1μm were grown from a hexagonally packed mask with 3 μm diameter holes with a center to center spacing of 9 μm. Larger wires with a radius of approximately 4 μm were grown from a hexagonally packed mask with 15 μm diameter holes and 30 μm center to center spacing.

After growth, the metal VLS catalyst was removed from the wires and the height and diameter of the wires were measured using scanning electron microscopy. The wires were embedded in polydimethylsiloxane (PDMS, Sylgard) as reported previously [19]. The PDMS was drop-cast onto the wires and spun at 3000 rpm, and then cured at 120 °C for 30 minutes. Wires were removed from the substrate by scraping the PDMS film with a razor blade. Integrated reflection and transmission measurements were performed with a custom- built 4 inch integrating sphere apparatus using a Fianium supercontinuum laser illumination source and a 0.25 m monochromator [1]. The absorption of each sample was determined from the wavelength and angle resolved transmission and reflection measurements [6].

We then input structural parameters, as determined by SEM, from these measured arrays into the model developed above. The PDMS embedding material was included in the model, but the PDMS/air interface was neglected. (The PDMS/air interface gives about 3% reflection).

#138520 - $15.00 USD Received 22 Nov 2010; accepted 25 Jan 2011; published 4 Feb 2011

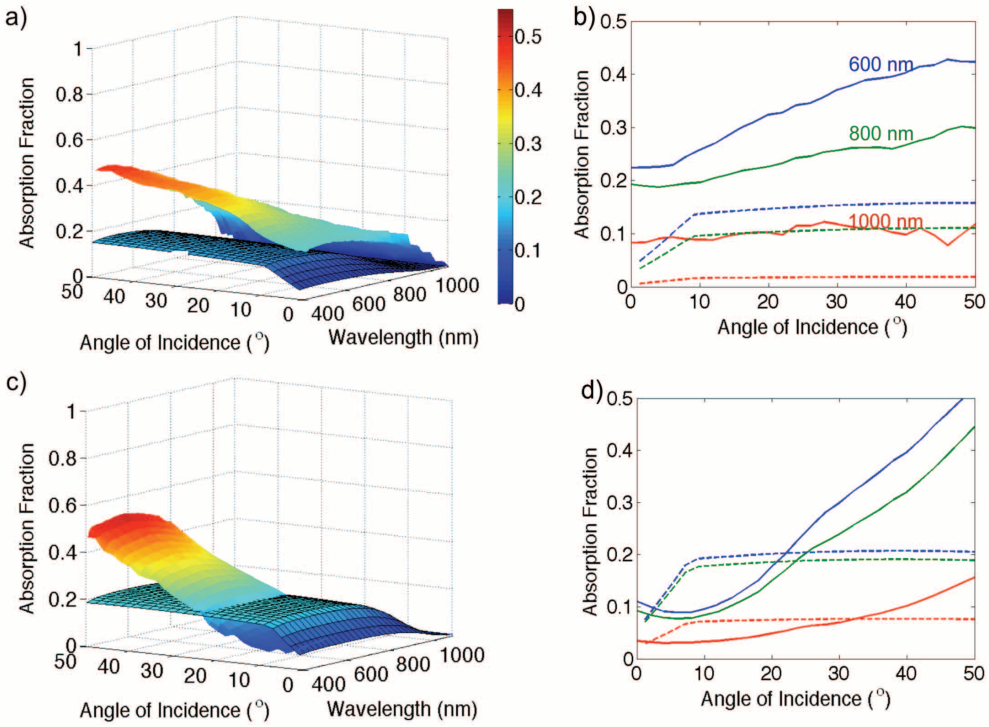

Fig. 5. (a)The outlined surface gives the model output for wires with a 4.9% filling fraction, a 1 μm radius, and a height of 44 μm. The upper surface is the experimental result for such an array. (b) The solid lines show the experimental data for various wavelengths, and the dotted lines show the model output. Note that even for the low absorbing 1000 nm curves, the model significantly underpredicts the absorption. (c) The outlined surface gives the model output for wires with a 7.3% filling fraction, a 4 μm radius, and a height of 160 μm. The other surface is the experimental result for such an array. (d) As before, the solid lines show the experimental data and the dotted lines show the model output. Note the reasonable agreement, especially at 1000nm.

For each angle of incidence and wavelength we found the various absorption and loss terms, using wavelength specific n and α data. For wires with an approximately 1μm radius, results are given in Figs. 5(a) and 5(b). We also compare to wires with a radius of approximately 4μm, and a similar aspect ratio, which should be closer to the ray optics limit. The results are shown in Figs. 5(c) and 5(d).

We found that the results for the larger wires are much more similar to the experimental data, though there is still significant disagreement. This suggests that there are significant wave optics effects in the 1μm radius case, which become less significant for the 4μm array. For example, if we examine the maximal absorption at near normal incidence we see that the model produces values similar to the filling fractions, and the 4μm array gives a value fairly close to the filling fraction with 11% absorption for a 7% filling fraction. However, for the 1μm array we see 23% absorption for a 5% filling fraction, suggesting a significant wave optic effect in this regime. In fact, it is well known that particles on the order of the wavelength of light can have scattering and absorption cross sections considerably larger than their physical size, whereas in ray optics the cross section corresponds to the physical size [20]. It seems likely that this effect is causing the enhanced absorption observed in the smaller wires.

#138520 - $15.00 USD
Received 22 Nov 2010; accepted 25 Jan 2011; published 4 Feb 2011

Despite the reasonable agreement for angles of incidence relatively near normal, the ray optics model fails to capture the strong increase in absorption observed with large angles of incidence for wavelengths where the absorption is strong. However, our model assumes that the light is fully randomized before any significant absorption takes place, which will not occur in strongly absorbing wavelength regimes. Thus, it is not surprising that our model fails to explain this behavior. As we expect, the agreement is improved for wavelengths where the absorption is low and this randomization condition is more accurate, as is shown in Fig. 5(d). However, even in this case, the shape of the curve is not captured particularly accurately, most likely due to differences between the experimental and modeled wires. For example, if the experimental wire surfaces were not perfectly Lambertian, but somewhat specular, the angular profile would likely be sloped across a wider range of angles, as is seen here. This is because the light which strikes the wire sides would reflect in one direction rather than be scattered in all directions, so light at near normal incidence would be less likely to enter the sides than for specular wires. Thus, our model works reasonably well in the low absorbing ray optics regime, but does not quite capture the angular dependence, perhaps due to non-Lambertian experimental wire surfaces.

7. Conclusion

The model developed in this paper addresses wire geometries from a ray optics perspective, assuming Lambertian surfaces and weak absorption. In the non-reflector case, the model produces light trapping close to the ergodic limit of n^2 for filling fractions approaching zero and approaching unity. This conforms with our thermodynamic expectation and allows us to understand the accuracy of the approximations used for computational feasibility. In addition, it confirms our physical expectations about the regimes for which the approximations will be most accurate.

Applying the model to the case of a Lambertian back reflector, we observe significant intensity enhancements, including asymptotic increases for small filling fractions that significantly exceed the ergodic limit of $2n^2$. Quantitatively, for a filling fraction of 0.1%, the enhancement can exceed $3n^2$, and the asymptotic increase goes approximately as $r^{-1/3}$, where r is the wire radius. These asymptotic increases result from the reflector acting as a concentrator with an acceptance angle of 2π steradian, and fitting them gives insight into the asymptotic behavior of the transmission factor for light that initially strikes the reflector, which goes as approximately $r^{5/3}$. It seems that a more sophisticated back reflector, which preferentially scattered sideways, could allow for asymptotic behavior which would be even more dramatic, a topic that deserves further study. However, while the asymptotic increases found here do give increased power per volume of silicon, there is reduced power per unit wire array area, owing to reduced silicon volume at low filling fractions.

Finally, in comparing the model with experimental absorption data, there is agreement with experiment for large (4 μm radius) wires in the low absorbing regime where the model is valid. The results suggest that the very strong absorption observed in smaller wires (1 μm radius) may be significantly due to wave optical effects, and analysis using a wave optics formalism is required in order to understand this strong absorption. Thus, even though previous modeling has suggested large wires could be superior from a device physics perspective, they appear to be less optimal from a light trapping perspective. This trade-off deserves further study, as do the wave optics effects observed in smaller wires.

Acknowledgements

The authors thank M. Kelzenberg for provision of data and insightful discussion, D. Callahan for advice on the manuscript and E. Warmann for assistance with figures. This material is based upon work supported as part of the Light Matter Interaction in Energy Conversion, an Energy

#138520 - $15.00 USD Received 22 Nov 2010; accepted 25 Jan 2011; published 4 Feb 2011

Frontier Research Center funded by the U. S. Department of Energy, Office of Science, Office of Basic Energy Sciences under Award Number DE-SC0001293.

#138520 - $15.00 USD Received 22 Nov 2010; accepted 25 Jan 2011; published 4 Feb 2011